Journal of Engineering and Technology
Vol. 1 No. 1 January – June 2013

Development of a Tracked Vehicle Robot with 3D Measurement System using Laser Range Finder

Toyomi FUJITA[#1], Yuya KONDO[#2]
[#]*Department of Electronics and Intelligent Systems, Tohoku Institute of Technology*
35-1 Yagiyama Kasumi-cho, Taihaku-ku, Sendai 982-8577, Japan
[1]t-fujita@tohtech.ac.jp
[2]hkondo@tohtech.ac.jp

Abstract - **This paper presents a tracked vehicle robot which has been developed in our laboratory and the "Embedded System Research and Development Center" of Tohoku Institute of Technology. The robot has two crawlers at the both sides. The crawler consists of rubber blocks, a chain and three sprocket wheels. The rubber blocks are fixed on each attachment hole of the chain. The robot therefore can move in a variety of field including rough terrain. We have also developed a novel 3D measurement system using a laser range finder with an arm-type movable unit. This system is mounted on the robot and enables the robot to measure variety of 3D configuration. Because of the occlusion can be avoided by this mechanism, the robot can measure a 3D configuration such as valley, gap, upward or downward stairs more accurately. Experimental results showed that proposed system is useful for sensing more complex terrain and applicable to variety of industrial technology area.**

Keywords - **Tracked Vehicle Robot, 3D Environment Sensing, Laser Range Finder (LRF), Embedded System**

I. INTRODUCTION

It is important to build robots that are able to work in rough terrain. For example, it is useful if robots may explore barbaric lands for the purpose of development. In addition, rescue robots need to operate properly in urban disaster areas caused by earthquake, fire, explosion, etc. Robots have to move flexibly in such rubble environments. We have therefore developed a tracked vehicle robot and have been studying on its movement and sensing system.

A 3D configuration sensing is a very important function for a tracked vehicle robot to give precise information as possible to operators and to move working field efficiently. A laser range finder (LRF) is widely used for a 3D sensing because it can detect wide area fast and can obtain 3D information easily. Some sensing systems have been presented as more accurate 3D sensing method using the LRF in earlier studies [1][2][3]. In those measurement systems, multiple LRF sensors are installed in different directions [4], or a LRF is mounted on a rotatable unit [5][6]. It is however still difficult for those systems to make sensing more complex terrain such as valley, deep hole, or inside the gap. As the other related work, for example [7], proposed the combination of 2D LRF and stereo vision for 3D sensing. This method however increases the cost of sensing system.

In this study, we propose a LRF sensing system that is able to sense such a more complex terrain: valley, deep hole, inside the gap. The system has an arm-type movable unit which can be mounted on a tracked vehicle robot. A LRF is installed at the end of the unit in this sensing system. The sensor can change position and orientation in a movable area of the arm unit and face at a right angle according to a variety of configuration. This system is therefore possible to avoid occlusions for such a complex terrain and sense more accurately.

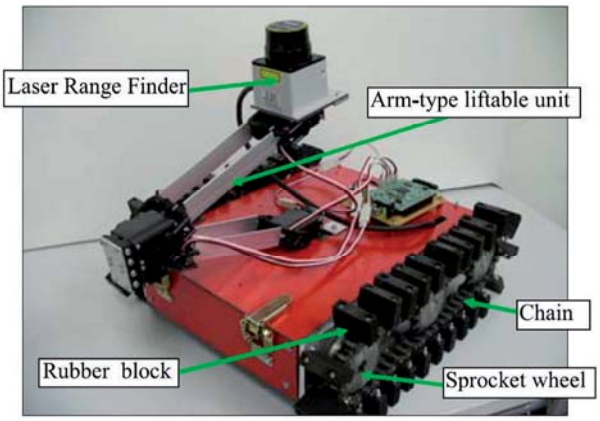

Fig. 1. Developed Tracked Vehicle Robot

We have designed and developed a prototype system of the movable LRF unit in addition to the tracked vehicle. In this paper, Section 2 describes an overview of the developed tracked vehicle and sensing system. Section 3 and 4 present experiments and results which were employed to confirm a sensing ability of this system.

II. DEVELOPMENT OF TRACKED VEHICLE ROBOT

This section describes an overview of a Tracked Vehicle Robot and 3D sensing system which we have been developing.

A. Main Robot

We have been developing a tracked vehicle robot which is able to work in rough terrain toward rescue activities. Fig. 1 shows an overview of the robot. The robot has two crawlers at the both sides. A crawler consists of rubber blocks, a chain and three sprocket wheels. The rubber blocks are fixed on each attachment hole of the chain. One of the sprocket wheels is actuated by a DC motor to drive a crawler for each side. In this mechanism, the robot can move in a variety of field including rough terrain. The size of the robot is 400[mm] (length) x 330[mm](width) x 230[mm](height), when the sensor is descended on the upper surface of the robot. This robot is controlled using an SH embedded micro computer.

B. Sensing System

We have designed a 3D sensing system which consists of an arm-type sensor movable unit and a LRF sensor. The prototype system has been developed and mounted on the tracked vehicle robot as shown in Fig. 1

The arm-type sensor movable unit has two links. The length of each link is 160[mm]. The links are connected by two RC servo motors as a joint in order to make the sensor horizontal orientation easily when folded. Another two joints are also attached to the both ends of the connecting links; one is connected to the sensor at the end

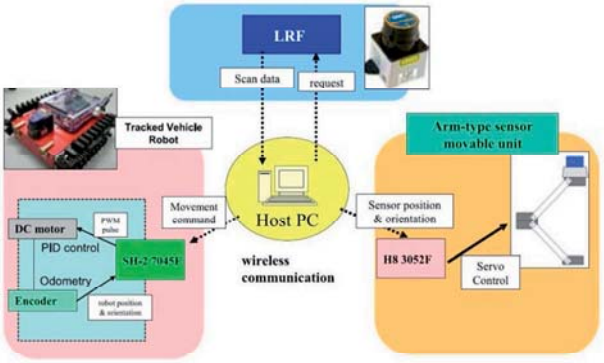

Fig. 2. Control System

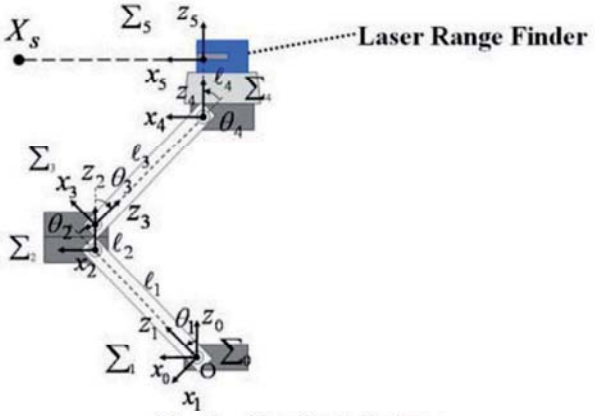

Fig. 3. Coordinate Systems

and the other is mounted on the upper surface of the robot. The robot can lift the sensor up to a height of 340[mm] and change its position and orientation by rotating those joints around *y* axis.

HOKUYO URG-04LX [8] is used as the LRF sensor in this system. This sensor can scan 240 degrees area and obtain distance data every 0.36 degree on a 2D plane. This sensor is equipped at the end of the arm-type unit and is able to change its position and orientation.

C. Control System

The control system of this robot consists of two embedded micro computers: Renesas SH-2/7045F and H8/3052F for controlling the main robot and the arm-type sensor movable unit respectively. Fig. 2 shows the control system. A Windows/XP host PC manages all controls of those units as well as scanned data of the sensor. The host PC sends movement commands to individual embedded micro computers for the robot and arm-type unit and request for sensor data acquisition to the sensor. The sensor can communicate directly with the host PC. All communications for those protocols are made by wireless serial communications using bluetooth-serial adapters: SENA Parani-SD100.

The embedded system has been developed in the "Embedded System Research and Development Center" of Tohoku Institute of Technology. The center was established in 2008 for the purpose of both of education and research on embedded system.

III. CALCULATION OF 3D POSITION

In this system, the robot can obtain 3D sensing positions from the sensor data of the LRF. We gave coordinate systems to each joint of the arm-type unit and

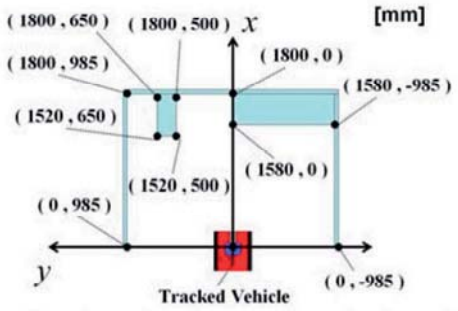

Fig. 4. Experimental environment for a simple configuration

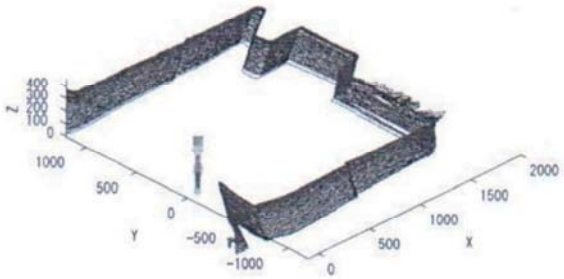

Fig. 5. Measurement result of a simple configuration

sensor as shown in Fig. 3 When the distance is d_s at a scan angle θ_s, the 3D measurement position vector $\boldsymbol{X}$ in the base coordinate system Σ_0 can be calculated by

$$\begin{pmatrix} \boldsymbol{X} \\ 1 \end{pmatrix} = {}^0\boldsymbol{P}_1 \; {}^1\boldsymbol{P}_2 \; {}^2\boldsymbol{P}_3 \; {}^3\boldsymbol{P}_4 \; {}^4\boldsymbol{P}_5 \begin{pmatrix} X_s \\ 1 \end{pmatrix} \quad (1)$$

where $\boldsymbol{X}_s$ shows a position vector of sensor in the sensor coordinate system Σ_s:

$$\boldsymbol{X}_s = d_s \, (\cos\theta_s, \sin\theta_s, 0)^{\mathrm{T}} \quad (2)$$

${}^i\boldsymbol{P}_{i+1}$ $(i = 0, \ldots, 4)$ shows a homogeneous matrix that represents a transformation between two coordinate systems Σ_i and Σ_{i+1}:

$${}^i\boldsymbol{P}_{i+1} = \begin{pmatrix} {}^i\boldsymbol{R}_{i+1} & {}^i\boldsymbol{T}_{i+1} \\ \mathbf{O_3}^{\mathrm{T}} & 1 \end{pmatrix} \quad (i = 0, \ldots, 4) \quad (3)$$

where ${}^{i}\boldsymbol{R}_{i+1}$ shows a rotation matrix for the rotation angle θ_{i+1} around y_i axis,

$$ {}^{i}\boldsymbol{R}_{i+1} = \begin{pmatrix} \cos\theta_{i+1} & 0 & \sin\theta_{i+1} \\ 0 & 1 & 0 \\ -\sin\theta_{i+1} & 0 & \cos\theta_{i+1} \end{pmatrix} \quad (4) $$

for $i = 0, \ldots, 4$, and ${}^{i}\boldsymbol{T}_{i+1}$ shows a translation vector from Σ_i to Σ_{i+1} : for the translation l_i on z_i axis:

$$ {}^{i}\boldsymbol{T}_{i+1} = (0, 0, l_i)^T \quad (5) $$

for $i = 0, \ldots, 4$ ($l_0 = 0$). $\mathbf{0}_3$ shows a 3 x 1 zero vector.

IV. EXPERIMENTS FOR 3D SENSING

We employed fundamental experiments to confirm basic sensing ability of the sensing system for simple environments: simple room and upward stairs. Additional experiments were also performed to confirm the usefulness of this sensing system for more complex environments: downward stairs, valley configuration and side hole configuration under the robot. The following sections describe those experiments and results.

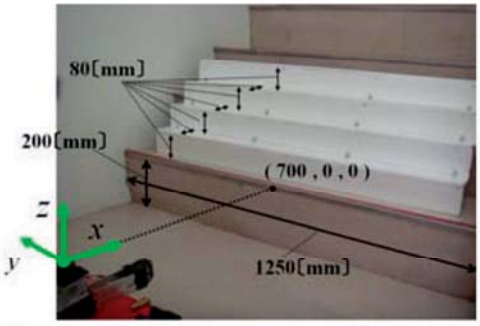

Fig. 6. Experimental environment for upward stairs

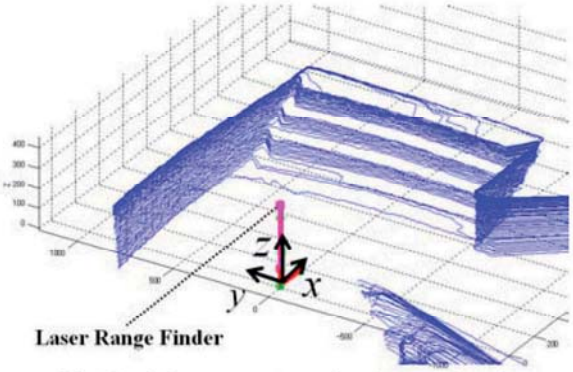

Fig. 7. Measurement result of upward stairs

A. Simple Room

A measurement of a simple room configuration were employed. Fig. 4 shows the experimental environment. The LRF sensor was lifted vertically from the upper surface of robot to the height of 340[mm] every 68[mm] by the arm-type unit. Each scanning of the sensor was performed for each height. We remotely controlled the height of the sensor in this experiment.

Figure 5 shows measured 3D shape. Comparison of the result with actual environment (Fig. 4) shows that the information of distance and shape to wall or object can be obtained almost accurately in this sensing system. The shape of left-front side for the robot can not be measured accurately because the area is occluded. The information of the area can be measured easily by moving robot and the arm-unit to the left side.

B. Upward Stairs

We employed a measurement of upward stairs as another experiment for basic environment. Fig. 6 shows the experimental environment. The stairs are located 700[mm] ahead of the robot. Each stair is 80[mm] in height and depth. The experiment was performed in the same manner as the previous experiment.

Figure 7 shows the measurement result; almost same configuration to actual environment was obtained in this sensing system.

C. Downward Stairs

3D measurements for downward stairs, shown in Fig. 8, were performed. Fig. 8(a) shows an overview of the experimental environment and Fig. 8(b) shows its schematic diagram with reference points, which we picked from some feature points for measurement error analysis. Each stair is 80[mm] in height and depth, as well as the previous experiment.

In this experiment, the robot stayed at one position, 330[mm] away from the top stair, and moved the arm-unit so that the sensor was located over the downward stairs. The sensor angle was changed by rotating the angle θ_4, shown in Fig. 3, with the same position of the end of the arm-unit by keeping the angles θ_1, θ_2, and θ_3.

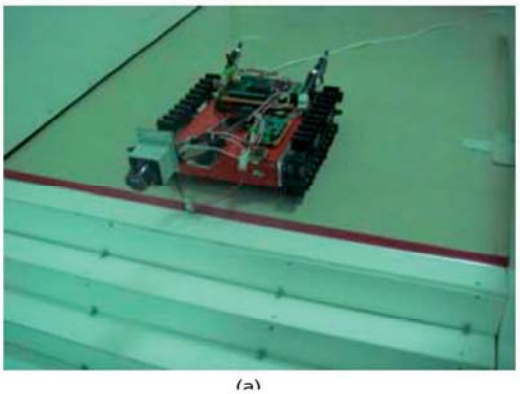

(a)

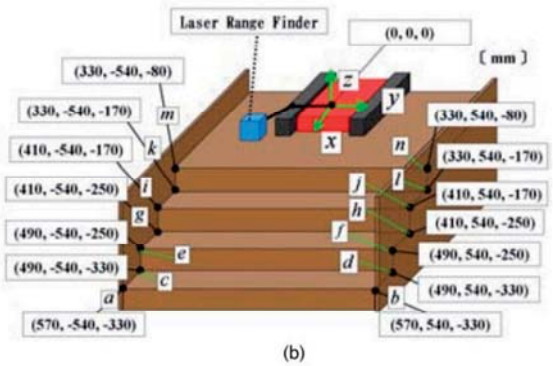

(b)

Fig. 8. Experimental environment for downward stairs (a):overview (b):schematic diagram with reference points

The rotation angle θ_4 was controlled remotely from 0

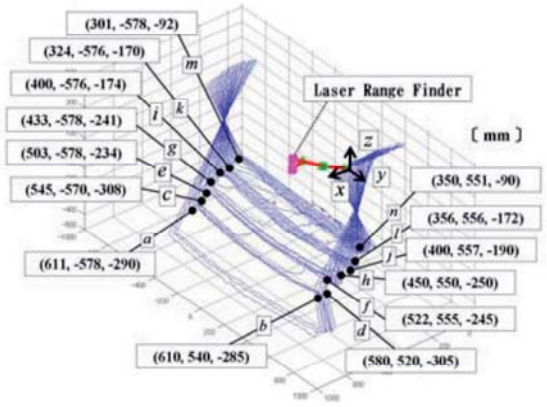

Fig. 9 Measurement result of downward stairs with measurement position values for reference points (unit: [mm])

degree to 60 degrees every 1.8 degrees. The scanning of the LRF was performed for each sensor angle. The sensing data were then accumulated to make 3D map.

Figure 9 shows the measurement result. We can see almost same configuration to actual environment. The measurement position values for reference points are also denoted in the figure. The position values show that accurate position can be sensed by this system. Table I shows actual and measured distance with error ratio values on the reference points. This result also confirms valid sensing of this system because error ratio values of the distance were within 5.8% for all reference points.

D. Valley

A valley configuration was set up as an experimental environment. Fig. 10(a) and Fig. 10(b) show overviews of the environment and Fig. 10(c) shows its schematic diagram. It was 610[mm] deep and 320[mm] long. We gave reference points at each corner of the configuration to estimate actual error value on measurement points. In the same way as previous experiment, the robot stayed at one position, 250[mm] away from the border, and the sensor was located over the valley by the arm-unit. The sensor angle only was changed and the other joints of the arm kept angles to be fixed sensor position. The rotation angle of the sensor, θ_4, varied from 0 degree to 90 degrees every 1.8 degrees. Each scanning was performed for each sensor angle.

TABLE I: MEASUREMENT DISTANCES AND ERROR RATIOS ON REFERENCE POINTS FOR DOWNWARD STAIRS

	distance [mm]			
point	actual	measured	error	error ratio [%]
a	851.7	889.7	38.0	4.5
b	851.7	863.1	11.4	1.3
c	800.4	846.6	46.3	5.8
d	800.4	836.6	36.2	4.5
e	770.8	801.2	30.3	3.9
f	770.8	800.3	29.5	3.8
g	722.6	761.4	38.7	5.4
h	722.6	753.3	30.7	4.2
i	699.0	722.5	23.5	3.4
j	699.0	711.6	12.6	1.8
k	655.3	682.4	27.1	4.1
l	655.3	682.2	27.0	4.1
m	637.9	658.1	20.3	3.2
n	637.9	658.9	21.1	3.3

Figure 11 shows the measurement result. We can see very similar configuration to the actual valley. The measurement position values for reference points are also denoted in the figure. The position values show that accurate position can be sensed by this sensing system. Table II shows actual and measured distance with error ratio values on the reference points. Even though the error ratio for the point *e* was higher, the most of the values are less than about 5% for the other points.

E. Side Hole Under Robot

We employed an experiment or measurement of a side hole configuration under the robot. Fig.12(a) shows an overvsiew of the experiment and Fig. 12(b) shows its schematic diagram. The dimension of the hole was set to 880[mm](width) x 400[mm](height) x 600[mm](depth). Eight reference points were given at each corner of the hole to estimate actual errors.

The robot stayed at one position as previous experiments and the sensor was located in front of the hole by the arm-unit. Each of joints except for the last joint to change sensor angle was rotated to fixed angle to keep the sensor position. The sensor angle, θ_4, only varied from 0 degree to 70 degrees every 1.8 degrees. Each scanning was performed for each sensor angle.

Figure 13 shows the measurement result. This result also showed almost same configuration to the actual environment. The measurement position values for reference points are also denoted in the figure. Table III shows actual and measured distance with error ratio values on the eight reference points. The error ratios demonstrated accurate sensing in this system; the maximum was 4.4% and average was 1.9% for all points.

V. DISCUSSIONS

We have employed fundamental experiments for sensing simple environment: a simple room and upward stairs, as described in Section 3. From Fig. 5 and Fig. 7, we can see that the almost same configuration was measured respectively. We therefore confirm that this sensing system has basic ability of 3D sensing. In addition, because the system can change the height of the sensor by lifting the end of the arm-unit at equal interval, we can avoid a problem on accumulation point in conventional method which uses a rotating mechanism.

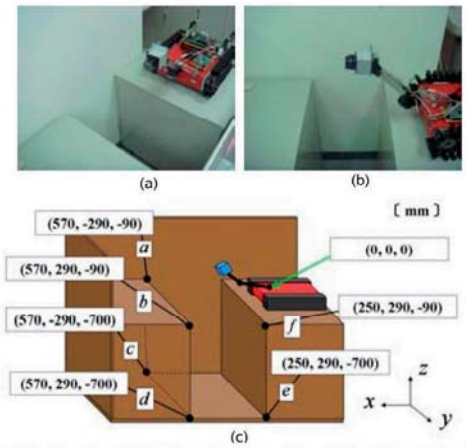

Fig. 10. Experimental environment for a valley configuration (a):front view (b):side view (c):schematic diagram with reference points

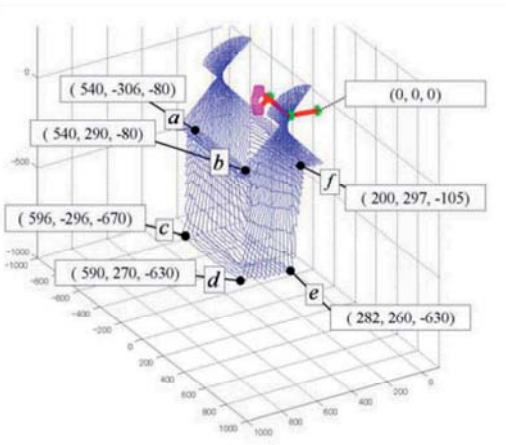

Fig. 11. Measurement result of a valley configuration with measurement position values for reference points (unit:[mm])

TABLE II : MEASUREMENT DISTANCES AND ERROR RATIOS ON FEATURE POINTS FOR A VALLEY CONFIGURATION

	distance [mm]			
point	actual	measured	error	error ratio [%]
a	645.8	625.8	20.0	3.1
b	645.8	618.1	27.7	4.3
c	948.2	944.3	3.8	0.4
d	948.2	904.4	43.8	4.6
e	797.9	737.6	60.3	7.6
f	393.3	373.1	20.2	5.1

Additional experiments described in Section 4 showed that this sensing system is also useful for more complex environment. The result of sensing for downward stairs, as shown in Fig. 9 and Table I, suggested that this system is possible to perform 3D mapping effectively even if the terrain has many occlusions. The error ratio of distance was about 5% at a maximum. We consider that this error value is acceptable for a mapping for the purpose of movement or exploration by a tracked vehicle or a rescue robot.

The 3D map of measurement result for a valley terrain, shown in Fig. 11, indicated another ability of the proposed sensing method. A robot can sense and make a map of deep bottom area safely by this method because the robot does not have to stand at close to the side of border. We consider that the error ratio of 7.6% for the reference point *e*, shown in Table II, occurred because the position was acute angle for the sensor. This error could be improved if the location of the sensor so that it can face to the right position to the point. This sensing system can correspond to variety of terrain because the arm-unit can provide a lot of position and orientation of the sensor.

The result of 3D measurement for a side hole under the robot also demonstrated another ability and strong advantage of the sensing system. Fig. 13 showed that this system enables us to obtain 3D information for such a shape which any conventional sensing system has never been able to measure. Moreover, the experimental result showed accurate sensing due to less error ratios, as shown in Table III. We therefore conclude this sensing system must be useful for 3D shape sensing specially in rough or rubble environments such as disaster area.

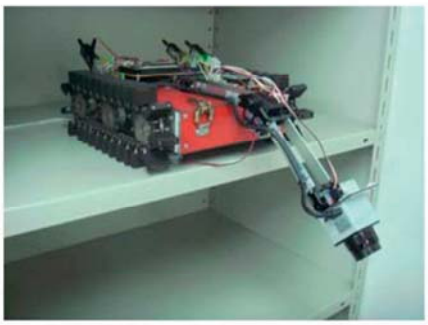

(a)

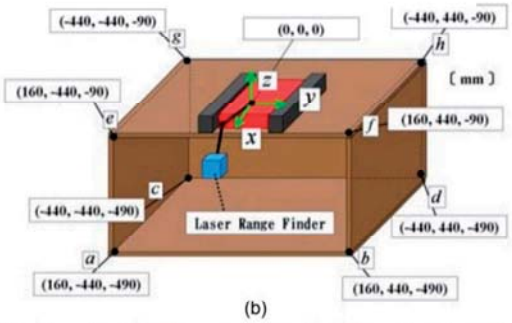

(b)

Fig. 12. Experimental environment for a side hole configuration under the robot (a):overview (b):schematic diagram with reference points

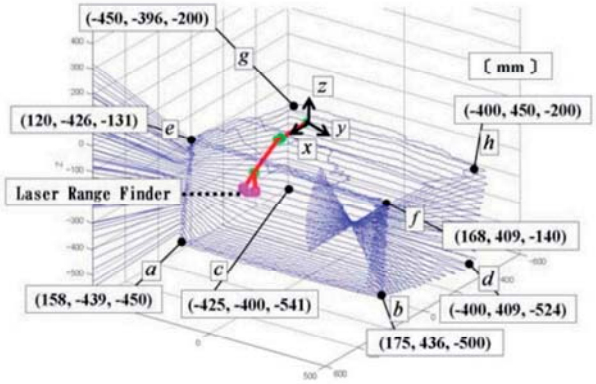

Fig. 13. Measurement result of a side hole configuration with measurement position values for reference points (unit:[mm])

TABLE III : MEASUREMENT DISTANCES AND ERROR RATIOS ON FEATURE POINTS FOR A SIDE HOLE CONFIGURATION UNDER THE ROBOT

	distance [mm]			
point	actual	measured	error	error ratio [%]
a	677.7	648.2	29.5	4.4
b	677.7	686.1	8.4	1.2
c	792.0	795.8	3.8	0.5
d	792.0	775.8	16.2	2.0
e	476.8	461.6	15.2	3.2
f	476.8	463.8	13.0	2.7
g	628.7	631.9	3.2	0.5
h	628.7	634.4	5.7	0.9

VI. CONCLUSIONS

This paper presented a tracked vehicle robot which has been developed in our laboratory and the "Embedded System Research and Development Center" of Tohoku Institute of Technology. In addition, a novel 3D sensing system was proposed for complex environment such as gap, valley, or downward stairs, which would be difficult to obtain correct information by conventional methods.

The experimental result showed that our method is useful for 3D sensing for such a complex environment. This robot is controlled using an SH embedded micro computer therefore students can easily use the robot and learn how to control a robot. We consider this robot and sensing system can be useful and applicable to variety of industrial technology area.

ACKNOWLEDGMENTS

The authors thank the "Embedded System Research and Development Center" of Tohoku Institute of Technology for generously providing facilities for development of the robot and experiments presented in this paper. This center is fully equipped for a practical lecture with teaching system for a professor and 50 PCs with embedded micro computer boards for students. Some research areas on embedded system—including robot system, network system, audio recognition system—are currently assigned in the center. Some graduate students including one of the authors were involved with the development of the robot system in the center. They have studied on robotics and mastered the skills of manufacturing embedded systems through the development in the desirable environment.

REFERENCES

[1] M. Hashimoto, Y. Matsui, and K. Takahashi, "Moving-object tracking with in-vehicle multi-laser range sensors," *Journal of Robotics andMechatronics*, vol. 20, no. 3, pp. 367–377, 2008.

[2] T. Ueda, H. Kawata, T. Tomizawa, A. Ohya, and S. Yuta, "Mobile SOKUIKI Sensor System-Accurate Range Data Mapping System with Sensor Motion," in *Proceedings of the 2006 International Conference on Autonomous Robots and Agents*.

[3] K. Ohno and S. Tadokoro, "Dense 3D map building based on LRF data and color image fusion," in *2005 IEEE/RSJ International Conference on Intelligent Robots and Systems, 2005.(IROS 2005)*, 2005, pp. 2792–2797.

[4] J. Poppinga, A. Birk, and K. Pathak, "Hough based terrain classification for realtime detection of drivable ground," *Journal of Field Robotics*, vol. 25, no. (1-2), pp. 67–88, 2008.

[5] A. Nuchter, K. Lingemann, and J. Hertzberg, "Mapping of rescue environments with kurt3d," in *In Proc. IEEE SSRR 2005*, 2005, pp. 158–163.

[6] Z. Nemoto, H. Takemura, and H. Mizoguchi, "Development of Smallsized Omni-directional Laser Range Scanner and Its Application to 3D Background Difference," in *Industrial Electronics Society, 2007. IECON 2007. 33rd Annual Conference of the IEEE*, 2007, pp. 2284–2289.

[7] L. Iocchi, S. Pellegrini, and G. Tipaldi, "Building multi-level planar maps integrating LRF, stereo vision and IMU sensors," in *Safety, Security and Rescue Robotics, 2007. SSRR 2007. IEEE International Workshop on*, 2007, pp.1–6.

[8] Hokuyo Automatic Co., Ltd., in *http://www.hokuyo-aut.co.jp*.